第51卷第11期 中国科学技术大学学报 Vol. 51, No. 11
2021年11月 JOURNAL OF UNIVERSITY OF SCIENCE AND TECHNOLOGY OF CHINA Nov. 2021
Received: 2021-04-21; Revised: 2021-08-09 doi:10.52396/JUST-2021-0114

Summer thermal performance study on pipe-embedded PCM composite wall in existing buildings

CHEN Sarula[1,4], CHANG Tianxin[1], YANG Yang[2*], PAN Chao[1], WU Yunfa[1,3,4]
1. College of Architecture and Urban Planning, Anhui Jianzhu University, Hefei 230601, China;
2. College of Architecture and Art, Hefei University of Technology, Hefei 230009, China;
3. State Key Laboratory of Fire Science, University of Science and Technology of China, Hefei 230027, China;
4. China-Portugal Joint Laboratory of Cultural Heritage Conservation Science, Suzhou 215031, China
* Corresponding author. E-mail: yangyang2017@tju.edu.cn

Abstract: Pipe-embedded building envelope is a heavyweight thermo-activated building system (TABS) that has its pipe circuits inside the building envelope, which has been seldom studied in existing buildings. In this context, the pipe-embedded PCM composite wall (PEPCW) in which the pipe-embedded interlayer is relocated to the outside of the load-bearing layer and replaced by macro-encapsulation-based pipe-embedded PCM panel is proposed to address the retrofitting challenges. In this paper, the summer thermal performance and energy saving potential of PEPCW are evaluated through a validated mathematical model. The simulation tests verify the effectiveness of PEPCW in cooling load reduction, and the corresponding amplitude value of interior surface temperature and heat flux can be decreased by 1.1 ℃ and 9.9 W·m^{-2}, respectively. Besides, the parametric tests indicate that the pipe interval has a more obvious influence than PCM thickness, and the value of 300/30 mm (pipe interval/PCM thickness) is recommended. Furthermore, the effectiveness of PEPCW is proved to be satisfactory in the three different cities (i.e., Tianjin, Nanjing, and Guangzhou), and the maximum heat gain reduction (i.e., 39.30 kWh·m^{-2}) is observed in hot summer and warm winter region (i.e., Guangzhou). In addition, the influence of solar absorbance on conditioned space at different orientations can be remarkably reduced through PEPCW, and the reduction in the three sunny sides are relatively higher than the dark side (i.e., north). Overall, the proposed PEPCW presents a satisfactory thermal behavior in the cooling season and could contribute to the progress of energy saving retrofit in the vast existing buildings.

Keywords: thermal performance; TABS; PCM; mathematical model; existing buildings
CLC number: TU111.4 **Document code**: A

1 Introduction

The building sector is one of the three major non-renewable energy consumers, causing about 40% of all terminal energy need around the world[1,2]. Statistics data shows that up to 50% of primary energy has been consumed to thermally regulate the heating/cooling load and condition indoor environment[3]. Actually, the external envelope, as an interface directly connects the inside and outside space, can highly affect the total energy demand and comfort feeling of users[4]. It should be noted that most of the existing buildings no doubt have a higher energy consumption rate than new-built buildings, especially those with a little or without any energy saving measures[5]. These affirm the urgency of exploring appropriate retrofitting measures to realize high-efficient existing buildings in either China or other countries.

Traditionally, insulating the building fabric and increasing the total thermal resistance is a common practice among designers and service engineers. This is usually effective in the heating season, however, it may also have a negative impact on heat dissipation in transition and cooling season when theoutdoorenvironment is suitable for exploiting the natural coldness resource (NCR). For example, Ji et al[6] reported that the dwelling buildings in the UK with a high level of insulation are often facing the problem of summer overheating, and the internal heat, therefore, has to be conditioned by chillers which no doubt would increase the energy consumption. Besides, increasing the insulation thickness is also limited by the aging and fire safety, lower heat capacity and the home builders' desire to provide maximum internal space[1].

Citation: Chen Sarula, Chang Tianxin, Yang Yang, et al. Summer thermal performance study on pipe-embedded PCM composite wall in existing buildings. J. Univ. Sci. Tech. China, 2021, 51(11): 840-856.

Nomenclature

T	temperature, ℃		*Greek symbols*
T_F	melting/solidifying temperature, ℃	ρ	density, kg · m^{-3}
T_e	outdoor temperature, ℃	ρ_s	surface absorptance, −
T_{in}	room temperature, ℃	λ	thermal conductivity, W · m^{-1} · ℃$^{-1}$
$T_{x=0}$	interior surface temperature	η	efficiency, −
$T_{x=L}$	exterior surface temperature	Γ_Φ	diffusion coefficient, −
R_{ES}	radiation heat exchange, W · m^{-2}	α	heat transfer coefficient, W · m^{-2} · ℃
H	pump head, m	θ_e	exterior surface temperature, ℃
G	design capacity, m^3 · h^{-1}	Φ	common variable
L	length, m		
c_p	specific heat capacity, J · kg^{-1} · ℃$^{-1}$		Abbreviation and subscripts
h	enthalpy, J · kg^{-1}	TABs	thermo-activated building system
U	velocity vector, −	PEPCW	pipe-embedded PCM composite wall
S_Φ	source term	GSHE	ground-source heat exchanger
r	volume liquid fraction, −	MRT	mean radiant temperature
L	latent heat, J · kg^{-1}	PVR	photovoltaic radiant panel
q	heat flux, W · m^{-2}	NCR	natural coldness resource
I	solar radiation, W · m^{-2}	PCM	phase change material
t	time, minute or hour	XPS	extruded polystyrene foam boards
b	thickness	ASHP	air-source heat pump
l/s	liquid/solid state of PCM	HVAC	heating, ventilation and air conditioning
U	velocity vector, −	ref	reference
S_Φ	source term	k/i	Water/ PCMs
r	liquid fraction, −	j	cement (j=1), XPS (j=2) and brick (j=3)

Thermal mass application is another common approach, which is functioning in dampening the temperature fluctuations within a building based on its ability to absorb and store heat. Among different thermal mass applications, PCM is regarded as a novel energy-saving approach due to its capacity of being able to store and release the heat to reduce the load caused by building envelopes[7]. It is reported that the energy storage capacity of a 5.0 mm PCM composite wall almost equals to an 8.0 cm thick concrete wall, and the energy storing capacity of a 1.5 cm thick gypsum-based PCM wall is 5-times higher than a usual gypsum board and equals to a 12.0 cm thick wall[8,9]. Meanwhile, macro-encapsulation PCM has been regarded as one kind of feasible package methods in building areas[10-13]. For example, Vicente et al[11] reported that the combination of macro-encapsulated PCM wall and 10.0 cm XPS external insulation could result in an 80% reduction of thermal amplitude. Despite the many advantages of PCM, the passive application of PCM is usually limited to a mild climate region where the external temperature is near to the melting/solidification zone[14,15]. That is why more than one kinds of PCM are integrated into the same building envelope to achieve year-round thermal management[16,17].

Therefore, new cost-effective alternatives to traditional thermal insulation and thermal mass approaches are required. The thermo-activated building system (TABs) appears to be an attractive technology by integrating the building structure to act as an energy-storage to make useful reductions in domestic energy use[18]. Primarily, TABs is a water-based regulating circulatory system coupled with the heavy building thermal mass (usually thick concrete slabs in ceilings or floors). And the replacement of the old air-based paradigm with water-based paradigm as well as the use of the building structure for energy storage is the two keys of TABs. Recently, the pipe-embedded building envelope in walls and windows, as a new type of heavyweight TABS, has gained increased attention[19,20]. Owing to its high efficiency under a small temperature difference condition, pipe-embedded building envelope greatly relaxes the restrictions on heat source temperature. This allows for the utilization of widespread close-to-free energy sources: e. g. solar energy, shallow geothermal energy and industrial waste heat in the heating season[21]; and NCR stored by ground source heat exchangers (GSHE) or radiate cooling through radiant panels in the cooling season[22,23].

For the pipe-embedded exterior wall, Zhou et al[19] reviewed the heat transfer calculation models of TABS and brought forward the early concept of the pipe-embedded building envelope coupled with GSHE and

solar collectors. They also developed different validated frequency-domain finite-difference (FDFD) models to predict heat transfer performances[24]. A thermal-water activated wall outfitted with mini-tube capillary-network is presented by Yu et al[25] and its transient thermal behavior influenced by water temperature and the flow rate was numerically examined in the summer condition. Their results supported the advantage of this type of composite wall in stabilizing the interior wall surface temperature and reducing the building energy consumption. Shen et al[26] utilized the air source heat pumps (ASHP), evaporative cooling (cooling tower) and natural heat sources (underground soil and water) as the source of low-temperature hot water or high-temperature cold water and comprehensive parametric studies (including climate regions, orientations, water temperatures) of the composite transparent/opaque building envelopes were conducted both in the heating and cooling season through numerical methods.

The pipe-embedded interlayer is usually not visible owing to the water-carrying pipes are placed inside the building envelope, which is of particular interest to architects[27]. Meanwhile, the above studies also have clearly highlighted the energy saving potential of the pipe-embedded building envelope. However, some limitations still exist in current studies and the application challenges of the pipe-embedded building envelope also will potentially prevent its large-scale promotion in practice. On the one hand, almost all previous studies focus on new-built buildings. Obviously, configurations of the pipe-embedded building envelopes for new-built buildings are not suitable for the existing buildings that lack the condition of reconfiguring its structures. Also, applications of the pipe-embedded building envelope in the current configurations usually presents a disadvantage in the aspect of malfunctions[28], making repairs difficult without major interventions on site. Though a closed pipe-embedded exterior wall system (with water pipe outside of the concrete layer) to harvest and absorb the solar heat gain in the south to intercept the heat loss in the north is proposed by Reference [21], this system can only play a limited role in a certain condition in the winter. On the other hand, the aforementioned studies on the pipe-embedded building envelopes have placed more focus on the thermal behavior and energy saving potential at the component level, and further savings and heat transfer enhancement through system operation control have merely been mentioned. Actually, the intermittent operation mode has been adopted in diverse fields including radiant ceilings/floors[18], which could effectively enhance the heat transfer and economic performance. It also should be pointed out that "clean energy heating/cooling" has earned abundant government supports especially in China that is suffering from serious air pollution[29]. Recently, a package of clean energy policies has been released by the Chinese government related to "peak-valley time-of-use price", "replacing heating coal with electricity" and "replacing heating coal with natural gas"[29], etc. These affirm the enormous potential of utilizing the pipe-embedded system with a cheaper electricity price during the valley period.

Despite the significant number of works in the literature dealing with the utilization of PCM in passive applications, not so many articles can be found on PCM in active building systems[30]. Current studies almost are all about PCM in ceiling panels or radiant floors[31-35]. Mazo et al[30] described a model developed to simulate a radiant floor system with PCM in simple building types. The PCM radiant floor model was based on a one-dimensional finite difference scheme where the effective capacity method is used for PCM simulation. To shift the cooling/heating load from the peak period to the off-peak period and also address the application problem of the radiant PCM floor in areas which both need cooling and heating in different seasons, Zhang et al[33-34] proposed and numerically studied a double layer PCM floor with different melting temperature. Koschenz et al[35] proposed a chilled ceiling panel coupled with PCM, this chilled ceiling panel device was designed to absorb a heat flux of 40 $W \cdot m^{-2}$ during 8.0 h without producing an increase in temperature above the comfort range. Therefore, the effectiveness of an active building system integrated with PCM for cooling and heating has been verified.

As illustrated in Figure 1, in this paper, a macro-encapsulated PCM based pipe-embedded composite wall (PEPCW) is proposed as a feasible and cost-effective energy saving retrofit idea for building designers and engineers, which can decrease the heat/cold loss through the building envelope in winter/summer by relocating the pipe-embedded interlayer to the outside of the load-bearing layer. To verify its effectiveness, an experimentally validated mathematical model has been developed to explore the transient summer thermal performance of the PEPCW and the corresponding potential to reduce the cooling load. Further, a comprehensive parametric study is carried out to reveal the influence of some key design parameters, including pipe interval and PCM thickness, which is useful for engineers and architects to evaluate the impact of these parameters on heat loss through practical PEPCW. Besides, the effect of the climate region and building orientation on the thermal performance is also evaluated. This research seeks to enrich the existing energy saving retrofit approaches for the vast existing buildings, supplement the current academic research in

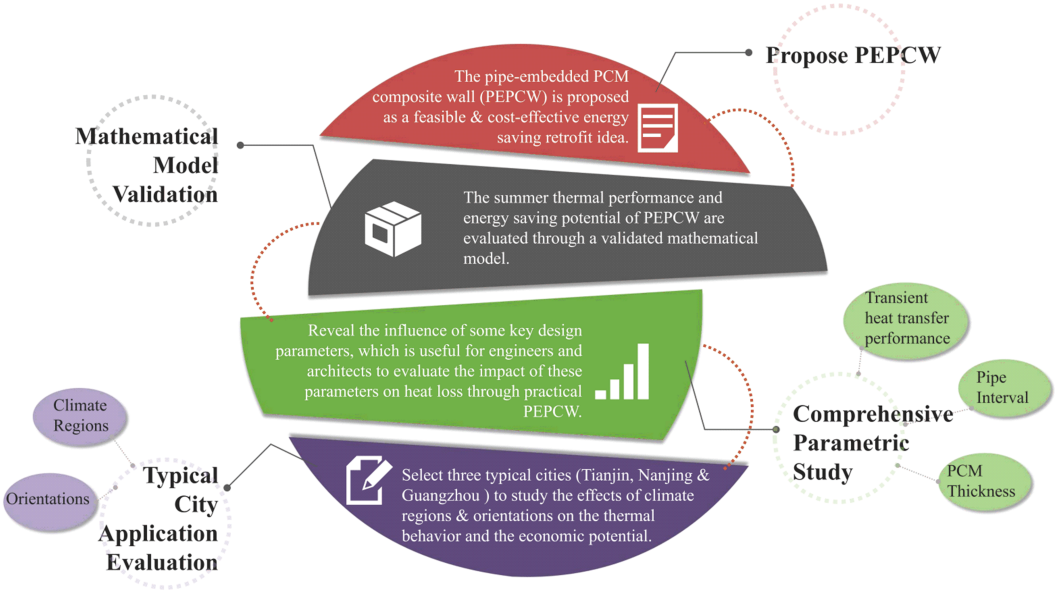

Figure 1. The main works done in the study.

the field of pipeline embedded building envelope structures, and provide the data and theoretical guidance for further research on PEPCW.

2 Mathematical model and validation

2.1 Geometric description

The PEPCW system basically consists of pipe-embedded PCM composite wall and local low-grade water source. In this paper, the embedded pipe is circulated with high-temperature cold water produced from GSHE or PVR during valley period to take away the heat inside of the wall and finish the coldness charging process simultaneously. As illustrated in Figure 2, the studied PEPCW is a typical 240 mm wall unit integrated with PCM interlayer and serpentine polythene pipes. The dimensions of the studied control volume are 2800 mm (length, i. e., room height), 350 mm (width, i. e., wall thickness) and 300 mm (height, i. e., pipe interval). The diameter of the embedded pipe is 20 mm. Due to the different U-value limit requirements in different climate regions[36], the insulation layer thicknesses for the three studied Chinese cities are 64 mm (cold/Tianjin), 36 mm (hot summer and cold winter/Nanjing) and 22 mm (hot summer and warm winter/Guangzhou). Macro-encapsulated organic paraffin RT24[37] through shaped aluminum plates is selected as the PCM interlayer. As such, modular production, installation and leakage risk of PEPCW could be well addressed and the building structure also would not be much affected. The material properties and geometric dimensions of PEPCW unit are given in Table 1.

2.2 Governing equations and boundary conditions

The three-dimensional heat transfer process of PEPCW is illustrated in Figure 2. In order to simplify the numerical process, some necessary assumptions are made as follows: ① Symmetry boundary conditions are considered between the serpentine pipes[21], as shown in Figure 2 (b); ② the longwave radiation heat exchange between the exterior wall surface and outdoor environment is considered in the form of sol-air temperature (T_o)[38]; ③ the thermophysical properties of materials are constant and they are thermally homogenous and isotropic except for the PCM in the phase change process[39]; ④ the thermal contact resistance between inner layers of PEPCW are ignored; ⑤ thermal expansion of PCM is neglected; ⑥ when the water inlet velocity is 0.5 m·s^{-1} from 23:00–06:00, it is the valley period that the PEPCW is deactivated (mass flow = 0), and the fluid inside the pipes is assumed to be a solid zone until 06:00–23:00 when the water velocity is 0 m·s^{-1}, PEPCW is reactivated (mass flow>0)[40].

The computation domain for PEPCW mainly consists of three parts (the PCM region, solid region and fluid region). For PCM region, two methods (enthalpy-porosity method and equivalent heat capacity method) are provided in Fluent solver in order to model the solidification/melting process[41]. Among them, the enthalpy-porosity method which determines the enthalpy value in the energy equation is proved to be better by numerically solving Navier-Stokes partial differential equations of mass, energy, and momentum[42,43]. The total enthalpy value covers both sensible and latent parts in which the latent enthalpy is evaluated as a percentage of the latent heat of

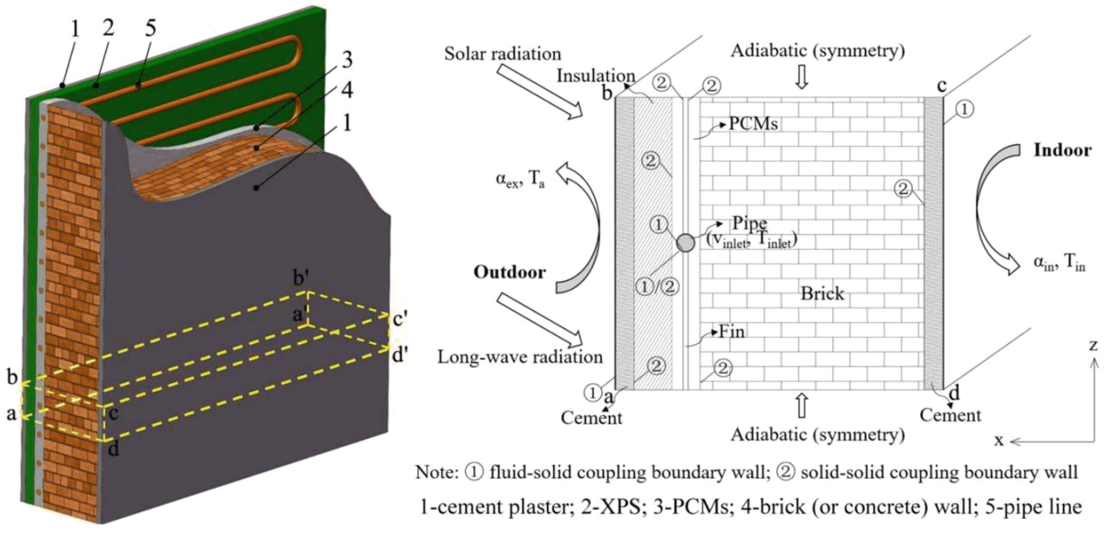

Figure 2. Geometry model and heat transfer process of PEPCW.

Table 1. Thermophysical properties and geometric size of PEPCW model.

Material	Density ρ ($kg \cdot m^{-3}$)	Thermal conductivity λ ($W \cdot m^{-1} \cdot ^{\circ}C^{-1}$)	Specific heat c_p ($J \cdot kg^{-1} \cdot ^{\circ}C^{-1}$)	Latent heat L ($kJ \cdot kg^{-1}$)	Thickness b (mm)	Melting/ Congealing T_F ($^{\circ}C$)
Cement plaster	1800	0.930	1050	/	20	/
XPS	30	0.042	1380	/	64 (Tianjin) 36 (Nanjing) 22 (Guangzhou)	/
Brick	1500	0.640	879	/	120	/
Copper pipe	8978	387.600	381	/	2	/
PCMs	880 (l) 770 (s)	0.200 (l) 0.200 (s)	2000	260	30, 40, 50	21–25 (l) 25–21 (s)
PCM container	2719	202.400	871	/	1	/

$$\rho_i \frac{\partial h}{\partial t} = \lambda_i \left(\frac{\partial^2 T}{\partial x^2} + \frac{\partial^2 T}{\partial y^2} + \frac{\partial^2 T}{\partial yz^2} \right) \quad (1)$$

where ρ is the density ($kg \cdot m^{-3}$), λ is the thermal conductivity coefficient ($W \cdot m^{-1} \cdot ℃^{-1}$), C_p is the specific heat capacity at constant pressure ($J \cdot kg^{-1} \cdot ℃^{-1}$) and h is the enthalpy ($J \cdot kg^{-1}$). The subscript i represents the PCM.

Further, the enthalpy of the PCM interlayer is computed as follows:

$$h = h_{ref} + \int_{T_{ref}}^{T} C_p dT + rL \quad (2)$$

where T_{ref} is the reference temperature when the specific enthalpy is zero ($T_{ref} = 0℃$). H_{ref} is the specific enthalpy at the reference temperature ($H_{ref} = 0$ $kJ \cdot kg^{-1}$). r is the local liquid fraction in the calculation region of PCM interlayer. L is the latent heat of PCM in the whole phase change process ($J \cdot kg^{-1}$).

Besides, the volume liquid fraction of the PCM domain is defined as:

$$r = \begin{cases} 0, \text{if } T < T_F(s) \\ 1, \text{if } T > T_F(l) \end{cases} \quad (3)$$

where T_F is the melting and solidifying temperature (℃).

For the solid area, the energy controlling equation is written as follows:

$$(\rho c_p)_j \frac{\partial T}{\partial t} = \lambda_j \left(\frac{\partial^2 T}{\partial x^2} + \frac{\partial^2 T}{\partial y^2} + \frac{\partial^2 T}{\partial yz^2} \right) j = 1,2,3 \quad (4)$$

where j represents the cement plaster ($j=1$), XPS ($j=2$) and clay brick ($j=3$), respectively.

For fluid area, the energy governing equation is given as:

$$\frac{\partial(\rho_k \Phi)}{\partial t} + \nabla(\rho \overline{U} \Phi) = \nabla(\Gamma_\Phi grad \Phi) + S_\Phi \quad (5)$$

The boundary condition for the interior surface is defined as:

$$\lambda \left. \frac{\partial T}{\partial x} \right|_{x=0} = \alpha_{in}(T_{in} - T_{x=0}) \quad (6)$$

where λ_0 ($W \cdot m^{-1} \cdot ℃^{-1}$) is the thermal conductivity coefficient of internal cement plaster. α_{in} ($W \cdot m^{-2} \cdot ℃^{-1}$) is the synthetic surface heat transfer coefficient, here the value is set to 8.7[44]. T_{in} is the indoor temperature setpoint (26 ℃) and $T_{x=0}$ (℃) is the interior wall surface temperature recorded in the Fluent solver.

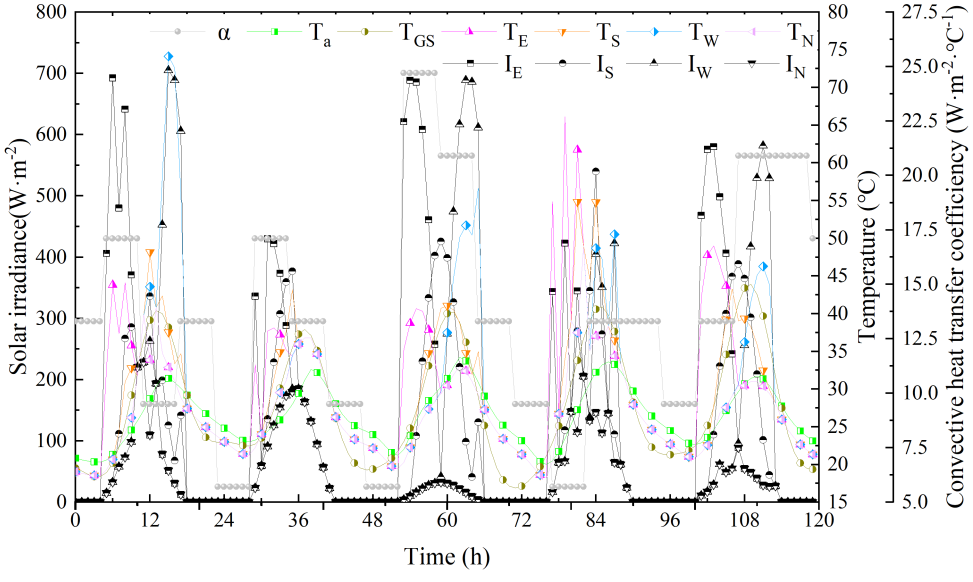

Appendix 1. Meteorological data of typical five days in Tianjin

For the boundary exposed to the ambient, it is defined as:

$$\lambda \left.\frac{\partial T}{\partial x}\right|_{x=L} = \alpha_{ex}(T_a - T_{x=L}) + \rho_s I - R_{ES} \quad (7)$$

where λ_L(W · m^{-1} · ℃$^{-1}$) is the thermal conductivity of external cement plaster. α_{ex}(W · m^{-2} · ℃$^{-1}$) is the exterior surface heat transfer coefficient, and the $\alpha_{ex}$is calculated by Eq. (8)[45]. T_a and $T_{x=L}$(℃) is the outdoor temperature and the exterior wall surface temperature, respectively. $\rho_s$is the external surface solar absorptance, which is 0.65 according to the Chinese code[46]. I (W · m^{-2}) is the solar irradiation. R_{ES}(W · m^{-2}) is the longwave radiation heat transfer between the external surface and ambient.

$$\alpha_{ex} = 5.62 + 3.9v \quad (8)$$

The sol-air temperature (T_o, ℃) is given as follows[46]:

$$T_o = \frac{I \cdot \rho_s}{\alpha_{ex}} + T_a \quad (9)$$

The boundary condition for the inside contact interfaces where there is no phase change transition to occur is defined as:

$$-\lambda \left.\frac{\partial T}{\partial x}\right|_{x,\text{layer1}} = -\lambda \left.\frac{\partial T}{\partial x}\right|_{x,\text{layer2}} \quad (10)$$

Otherwise, the boundary condition for the contact interface is given as:

$$-\lambda \left.\frac{\partial T}{\partial x}\right|_{x,\text{layer1}} = L\rho_j \frac{\partial r}{\partial t} - \lambda \left.\frac{\partial T}{\partial x}\right|_{x,\text{layer2}} \quad (11)$$

2.3 Numerical procedure

The numerical computation is carried out with the commercial CFD software, i. e., Fluent. Before the simulation, grid independence has been checked, and the total element and the node number of the PEPCW unit are 112750 and 119340, respectively. The governing equations are discretized by the second-order upwind scheme for advection terms and central differencing scheme, and the coupling of the velocity and pressure fields was carried out by using the SIMPLE algorithm. Due to the turbulence of cycling water, the standard $k-\varepsilon$ model (STD$k\varepsilon$) coupled with enhanced wall treatment (EWT) method is employed. All the meteorological data used in the simulation in the full text are from the special meteorological dataset for building thermal environment analysis of China[46]. Among them, the transient thermal performance of the TAPCW system in section 3.1 and a parametric study about pipe interval and PCM thickness in section 3.2 was firstly evaluated under Tianjin climate scenario. Correspondingly, the chosen meteorological data (i.e., solar irradiance, outdoor environment temperature and wind velocity) and calculated sol-air temperature from August 9 to 13 in Tianjin is showed in appendix 1. Following that the whole cooling season evaluation was taken in to account to evaluate the influence of climate and orientation of three typical cities in section 3.3 and 3.4. The cooling season in the mentioned three cities is May 22- Sep. 09 (Tianjin, 111 days), Jun. 03- Sep. 24 (Nanjing, 114 days) and May 13 - Oct. 19 (Guangzhou, 160 days), respectively. For details of the meteorological data is showed in appendix 2. During the simulation, the water temperature is 21 ℃ and the velocity is 0.5 m · s^{-1}. The characteristic change inside of the water zone as well as the boundary conditions is accomplished automatically through recorded journal-files and user-defined functions (UDF). The time step size is defined as 15 seconds and the boundary

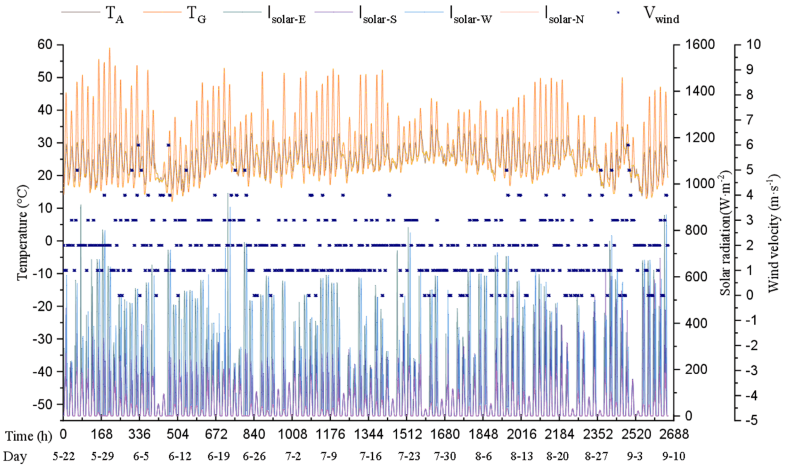

(a) Tianjin meteorological data

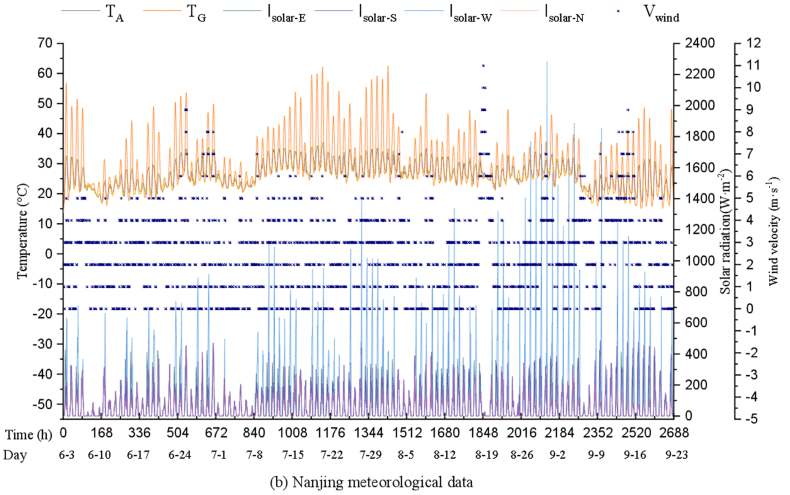

(b) Nanjing meteorological data

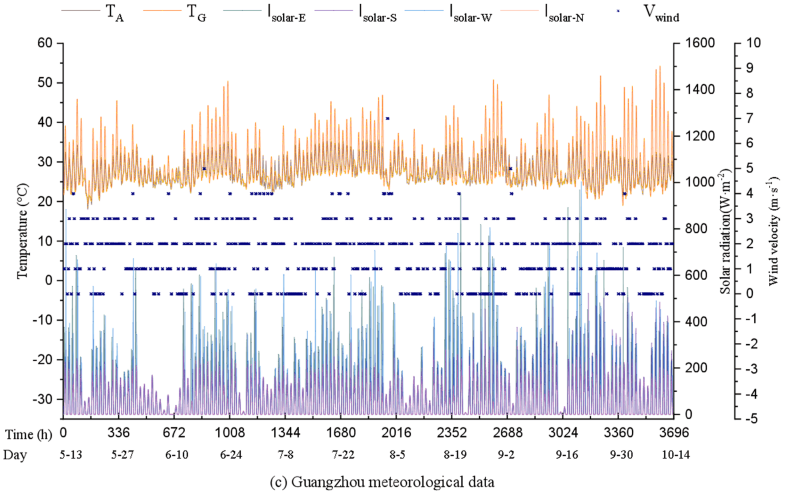

(c) Guangzhou meteorological data

Appendix 2. Meteorological data for three typical cities

conditions are changed every 60 minutes according to the available meteorological data. The convergence criteria are 10^{-7} for the residuals of the energy equation. To eliminate the thermal storage effect on the simulation results, the simulation for all of the cases has already calculated 5 days before the actual starting date[10].

2.4 Model validation

To verify the numerical model of PEPCW, a validation test is done and compared with the experiment result and simulation results presented in Reference [48]. Figure 3 shows a pipe-embedded PCM hot water wall mainly used for indoor radiant heating. The PEPCW studied in

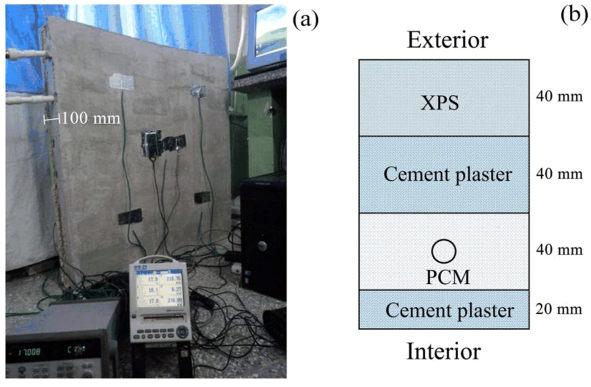

Figure 3. Test rig (left) and configuration of the radiant PCM wall (right) for validation.

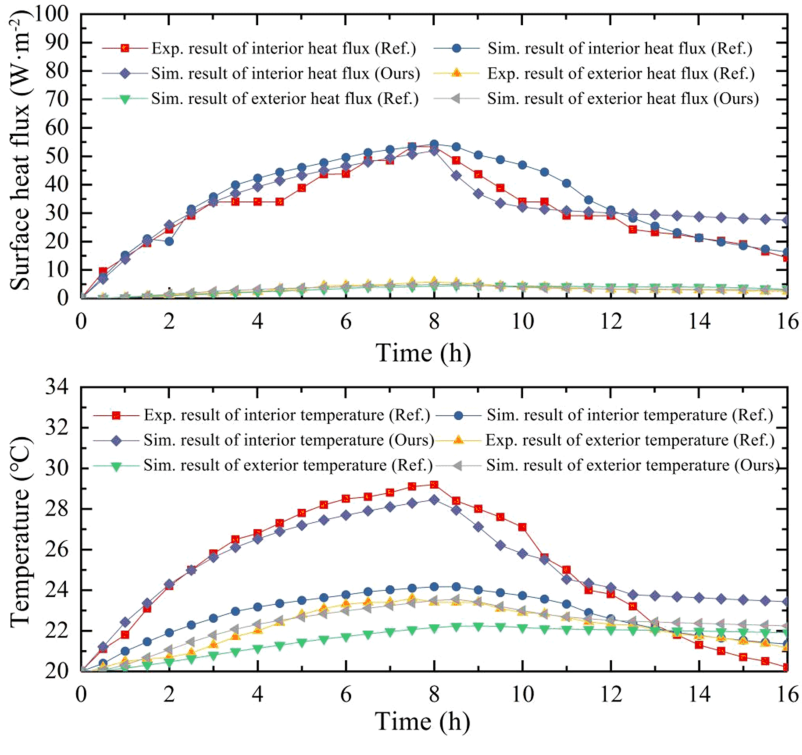

Figure 4. Comparison of the numerical and experimental results.

this paper is similar to the pipe-embedded PCM hot water wall in the aspect of structure, heat transfer process and boundary conditions. Usually, the parameter change (including the position, thermophysical and geometric) of the non-core structural layer has a slight impact on the numerical model. For the research object that has a similar heat transfer process and boundary conditions, lots of researchers have adopted this method in their parametric studies and comparative studies[26]. As shown in Figure 3 (a), the dimension of the experimental radiant wall unit is 1000 mm× 1000 mm× 100 mm. The test wall unit consisted of a 40 mm XPS (exterior) followed by two layers of cement plaster that are 40 mm and 20 mm thick with a 40mm layer of PCM layer between them. The PCMs adopted in the referenced test is the mixture of 48# solid paraffin and liquid paraffin provided by Sinopharm Chemical Reagent Beijing Co., Ltd, and the melting temperature and latent heat of fusion are 27.8 ℃ and 145.4 kJ · kg^{-1}. The external diameter and internal diameter of the PE pipe are 20 mm and 17.4 mm, respectively. The pipe interval is 150 mm. During the whole indoor test period, the indoor air temperature is kept constant at 20 ℃. 10 thermocouples and multi-point heat flow meter (KEM-HFM-215) distributed as Figure 3 (b) are fixed at both side of the interior and exterior surface to monitor the dynamic temperature and heat flux profile during the test. The initial temperature of the test wall unit is 20 ℃. The whole intermittent operation test lasts 16 hours with a continuous hot water

charging (50 ℃) during the first 8 hours.

Regarding the validation, a geometry model with the same dimensions of experimental test rig of Huo[48] is built in ANSYS. After that, the numerical results of the validation test are validated against both the experimental and numerical data. As can be seen in Figure 4, both the heat flux and temperature at the interior and exterior surface keep the same trend and agree well with the experimental result. Also, the simulation results obtained by us have an obvious improvement compared with that of Huo[48]. However, there also exists some difference between the experimental and numerical (ours) results. Taking their experimental results as the benchmark, the average relative value of the temperature and heat flux at the interior/exterior surface are 4.1%/2.7% and 17.4%/14.4% respectively. Compared with the average relative value of temperature, the relative value of heat flux is bigger. It should be noted that the value difference in the first 12 h is obvious than the last 4 h, which indicates that the calculation precision is different at different times. This could be attributed to the reasons as follows: (1) the thermophysical properties of the PCM given in the literature is not exactly accurate, especially in the melting/solidification temperature range, which may result in the value difference in heat charge/discharge process; (2) the installation error and cavities inside the PCM layer cannot be avoided in the experimental test especially for a macro-encapsulated PCM application, which may also change the equivalent thermophysical properties of PCM as the PCM layer is treated as an ideal PCM region without any thermal expansion or cavities in the simulation. In view of that, the accuracy of the numerical model is satisfying for engineering application with a macro-encapsulated PCM interlayer. The model can be used to study the thermal behavior of PEPCW and carry out parameter studies.

3 Results and discussion

3.1 Transient heat transfer performance analysis

In this section, the composite wall in south orientation is examined as an example in a typical day in the hottest month of Tianjin (Aug 13, the meteorological data is showed in appendix 1). It should be noted that a five day's simulation is conducted in all studied cases and only the results the last cycle are used for further analysis. For the PEPCW wall, the pipe interval is 300 mm and the PCM thickness is 30 mm. Hourly variations of surface heat flux, temperature and the liquid fraction inside of the PCM layer are presented in Figure 5. When the interior surface heat flux is negative, it means that the thermal energy is released to the indoor space, which is the so-called building cooling load. Conversely, when this value is positive, it states that the interior surface temperature is lower than the indoor setting point and therefore it absorbs heat from the room space, representing a supplementary cooling process. As is shown in Figure 5 (a), the interior surface of PEPCW is significantly 'decreased' during the simulation test and the maximum value difference of interior heat flux between the PEPCW and the ordinary wall is up to 9.9 W·m^{-2}. It could be found in Figure 5 (b) that the PEPCW exhibits a much lower maximum interior surface temperature. In detail, the peak value of the interior surface temperature decreased by 1.1 ℃ compared with the ordinary wall. It also could be observed that the interior surface temperature of the ordinary wall shows a time lag of 12 h, which usually causes extra and unnecessary cooling measures during the nighttime due to the higher mean radiant temperature (MRT). With the pipe-embedded PCM layer, the interior surface temperature is lower than 26 ℃ throughout the test, which means the MRT could be significantly reduced. Consequently, the PEPCW system could not only cut down the energy consumption

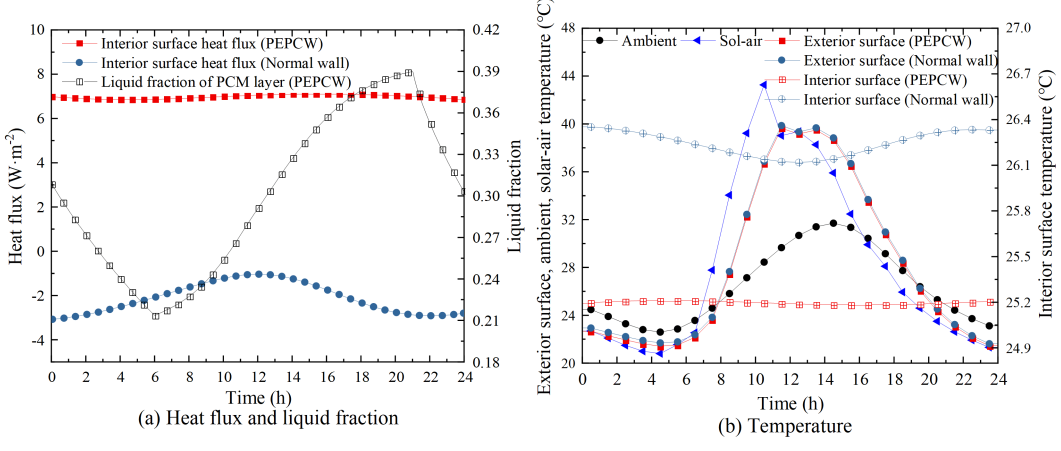

(a) Heat flux and liquid fraction (b) Temperature

Figure 5. Heat flux and temperature variation of the PEPCW.

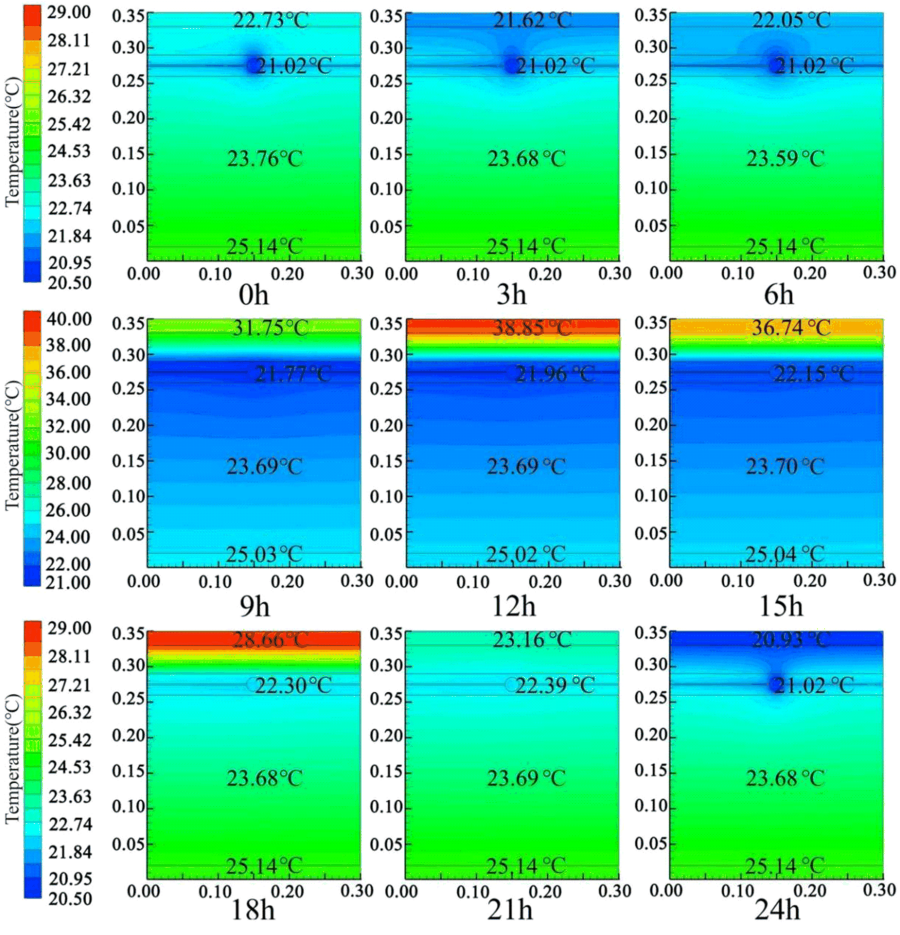

Figure 6. Variation of the temperature field at the cross-section of PEPCW.

but lift the indoor thermal comfort level at the same time. Results also show that the PCM inside of PEPCW could keep a dynamic balance during the test. And this could be regarded as another evidence of the effectiveness of PEPCW in building energy management because a stable melting/solidification cycle is a key index to evaluate the effectiveness of the PCM application. In a word, the PEPCW could act as a thermal barrier role between the indoor and outdoor environment, offsetting the heat gain through the building envelope and even supplying cooling energy to the indoor space. Accordingly, the initial investment and operating costs for a traditional HVAC system could be reduced correspondingly.

The variation of the temperature field at the cross-section of PEPCW is illustrated in Figure 6. It could be found that an obvious thermal stratification phenomenon of the composite wall is shown in the pipe-embedded zone. Temperature difference between the external cement and PCM layer varied from −0.1 ℃ to 16.9 ℃, while this value between the internal cement and PCM layer is within the range of 1.6−4.1 ℃. This implicates that the heat absorbed from the ambient can hardly pass through the PEPCW, thereby the interior surface temperature could be effectively controlled. Meanwhile, Figure 7 shows the temperature profile variation of the PEPCW and ordinary wall, where the dotted line (except for the monitoring points) is an indirect reference and not a direct simulation monitoring result. It could be seen that the temperature of the PCM layer remain at the melting/solidification zone throughout the whole day. The pipe-embedded PCM interlayer could significantly diminish the amplitude of temperature swing at the right side of PCM layer, making the temperature variation go flat between x = 0.09 m and x = 0.35 m, while the temperature profile in the left side does not decline seriously. This also indicates that relocating the pipe-embedded interlayer to the position between the load-bearing layer and the external XPS is technically feasible.

3.2 Effect of pipe interval and PCM thickness

Following the last section, the influence of pipe interval and PCM thickness under Tianjin condition is evaluated here. Figure 8 shows the heat flux and temperature variation of the interior surface as well as the liquid fraction inside of the PCM layer under different pipe interval and PCM thickness conditions. In Figure 8, the interior surface temperature for all of the nine studied

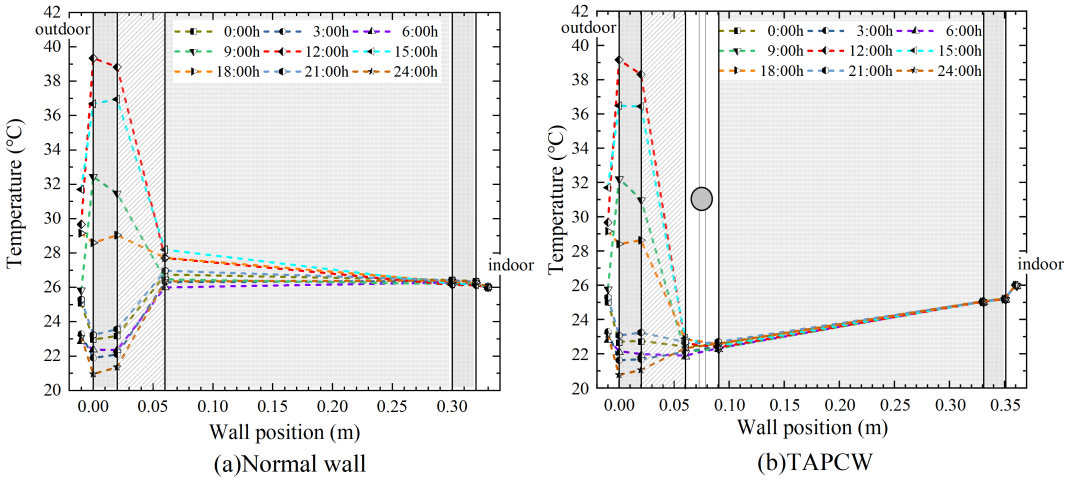

Figure 7. Temperature profile variation for the normal wall and PEPCW.

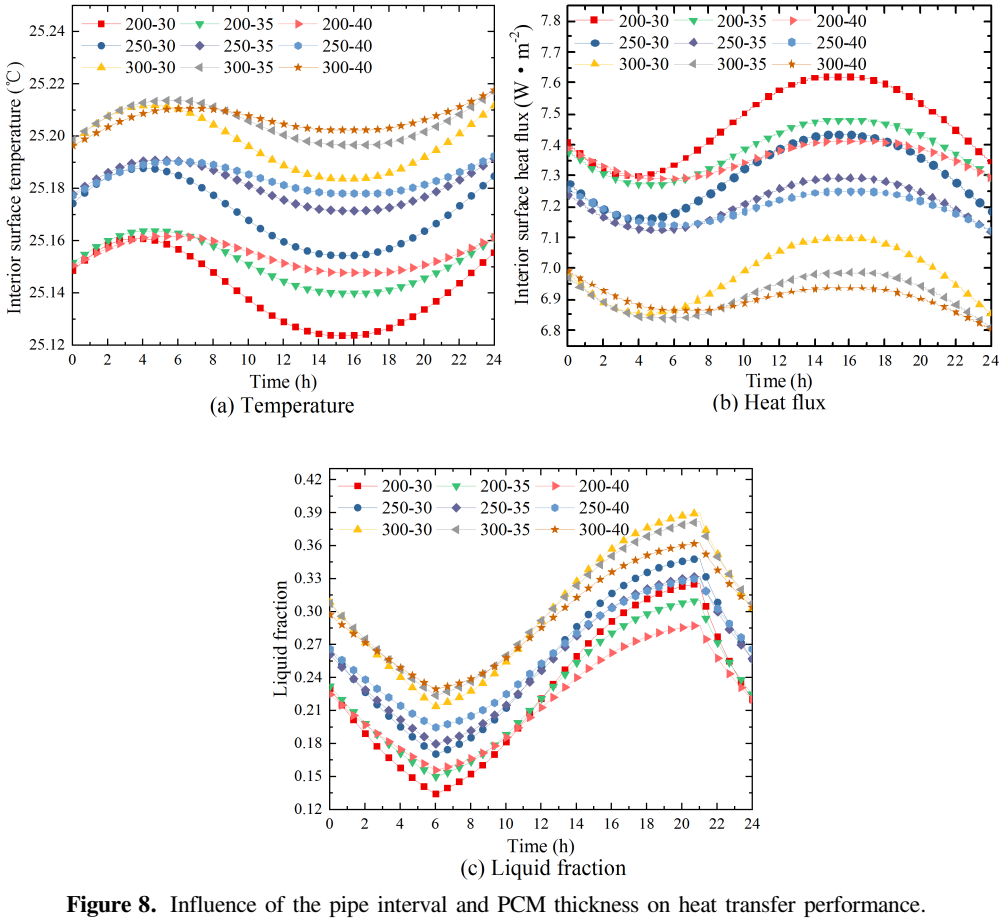

Figure 8. Influence of the pipe interval and PCM thickness on heat transfer performance.

cases are both lower than that of the indoor setting point and the interior surface heat flux is positive during the test, which means the nine studied cases are all effective. Further observation shows that when keeping PCM thickness constant and increasing the pipe interval, the interior surface temperature is also increased but the increment is reduced gradually. When keeping the pipe interval constant and increasing the PCM thickness, the interior surface temperature is increased instead of decreasing. The heat flux variation of interior surface in Figure 8 (b) also shows the same phenomenon. This could be probably attributed to the thermal conductivity of PCMs, which is lower than the bricklayer and the cement layer. That is to say, increasing the PCM thickness will also increase the thermal resistance between the pipe and the interior surface. Actually, a

lower thermal conductivity coefficient is desirable for energy-saving of ordinary buildings, because the heat transfer resistance is raised. Whereas, for PEPCW with intermittent thermal storage, both the heat transfer intercepting capacity and heat charge/discharge capacity are crucial. Besides, as is shown in Figure 8 (c), though steady phase change process occurs in all cases, a thinner PCM shows a higher utilization ratio. Therefore, though a thick PCM layer represents a higher energy storage potential, the balance between the heat charge/discharge and thermal intercepting capacity should be taken into account simultaneously, or it would be count-productive and also would bring in unnecessary material waste.

The impact of the pipe interval and PCM thickness on daily heat gain is illustrated in Figure 9. Results show that the daily accumulated heat gain of PEPCW is far less than the traditional one. For the ordinary wall, this value is positive and is around 0.05 kWh · m^{-2}, while these value for the studied PEPCW are both negative. Compared with the ordinary wall, the reduction ratio of this value is around 427.9-454.9% for PEPCW. Besides, though a closer arrangement of the embedded pipe and a thinner PCM layer shows a smaller accumulated heat gain value, the maximum percentage difference between the case of 200−30 and case 300−40 is only 27 which is not obvious compared with the overall decline ratio. As a result, a thinner PCM layer of 30 mm and a larger pipe interval of 300 mm are recommended here.

3.3 Effect of climate region

As is shown in appendix 2, different cities located in different climate region usually have different thermal insulation requirement and cooling demand. In this section, three typical Chinese cities are selected to evaluate the thermal performance of PEPCW. The three cities are Tianjin (cold region; latitude: 39.12° N), Nanjing (hot summer and cold winter region; latitude: 32.03° N) and Guangzhou (hot summer and warm winter region; latitude: 23.13° N), which distribute from south to north in China. Thus, cities in other countries have similar latitude or climate characteristic could also find valuable references in practice.

As is shown in Figure 10, the interior surface heat flux of PEPCW in three typical cities, compared with the ordinary wall, are both turned into positive and remain in a relatively stable status in the cooling season. Meanwhile, the interior surface temperature also could be controlled below the indoor setting point, which is beneficial for improving the indoor thermal comfort level. Figure 11 shows the monthly accumulated heat gain and the corresponding reduction of PEPCW. The simulation results state that when a higher heat gain is formed in a cooling month, a greater heat gain reduction will also be obtained. Therefore, though the heat gain varies greatly in different months of the cooling season, the PEPCW system could satisfy the heat gain reduction demand well and even provide extra cooling for the indoor space. Besides, due to the different primary meteorological conditions in different regions, the amount of heat reduction required for the building to achieve indoor thermal comfort is different. For areas with higher temperatures, the demand for heat reduction is higher; places with lower temperatures have the lower need, so the adjustment effect of TAPCW varies in different climate regions. The result shows that the total

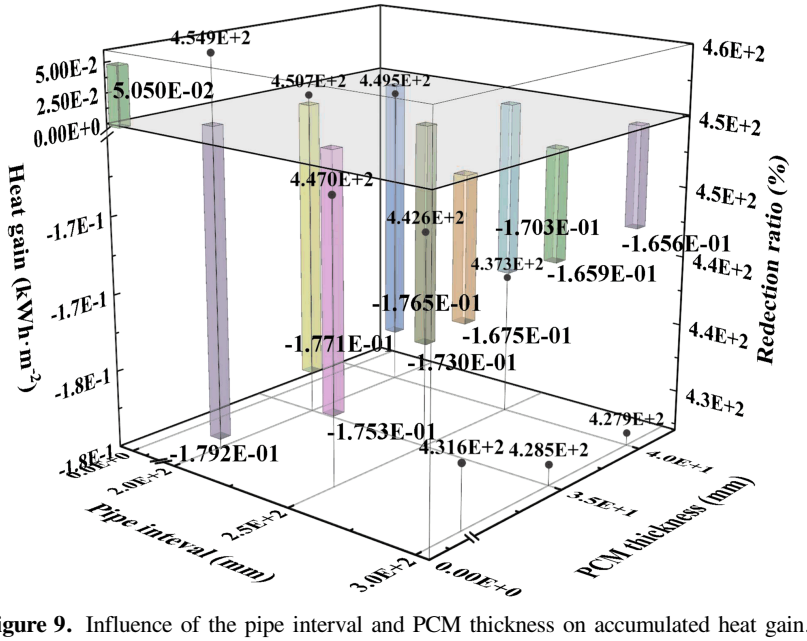

Figure 9. Influence of the pipe interval and PCM thickness on accumulated heat gain.

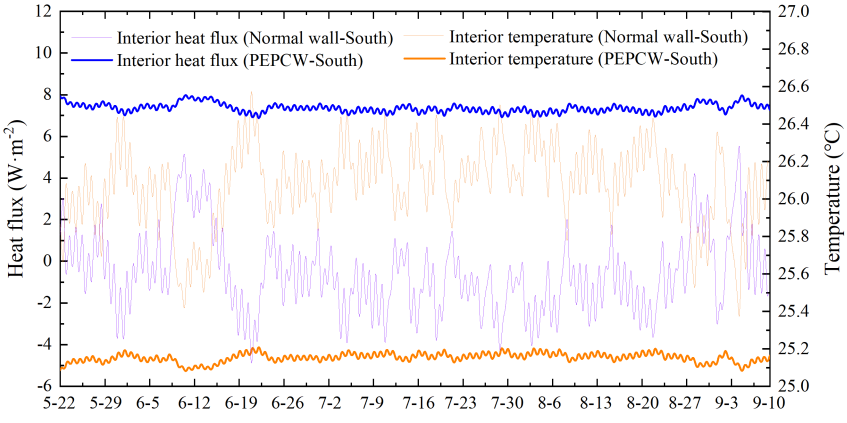

(a) Tianjin (cold climate/ latitude: 39.12° N,longitude: 117.20° E)

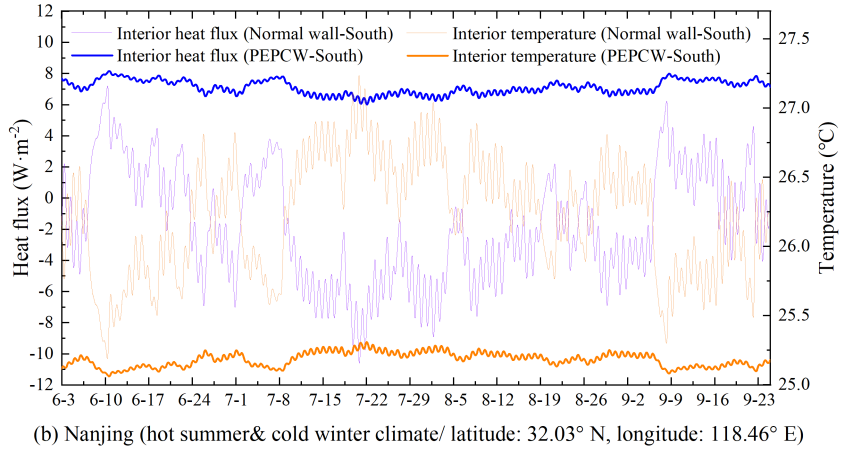

(b) Nanjing (hot summer& cold winter climate/ latitude: 32.03° N, longitude: 118.46° E)

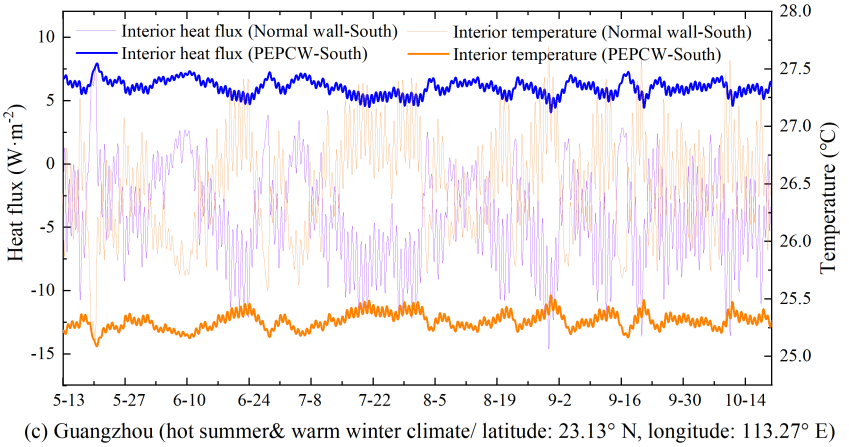

(c) Guangzhou (hot summer& warm winter climate/ latitude: 23.13° N, longitude: 113.27° E)

Figure 10. Hourly variation of the interior surface heat flux and temperature in typical cities.

heat gain of the ordinary wall in Tianjin is the smallest one (i. e., 1. 69 kWh · m^{-2}), and this value for Guangzhou application is the highest one (i. e., 16. 10 kWh · m^{-2}). While, for PEPCW, the heat gain of Guangzhou is lower than that of Tianjin and Nanjing, but their difference is not too much. The maximum heat gain reduction appears in Guangzhou, i. e. ,39. 30 kWh · m^{-2}, and the heat gain reduction in Tianjin and Nanjing is similar. Therefore, the PEPCW system is proved to be satisfactory in all of the selected cities.

3. 4 Effect of orientation

The solar radiation varies with the building orientation, which usually brings about the different thermal impact on the exterior wall for different orientations as well as the indoor environment. Thus, the impact of orientation on PEPCW is investigated in this section. Figure 12 show the orientation influence on heat gain and the corresponding reduction in typical cities. It could be seen that the accumulated heat gain of the ordinary wall at different orientations is significantly affected by solar

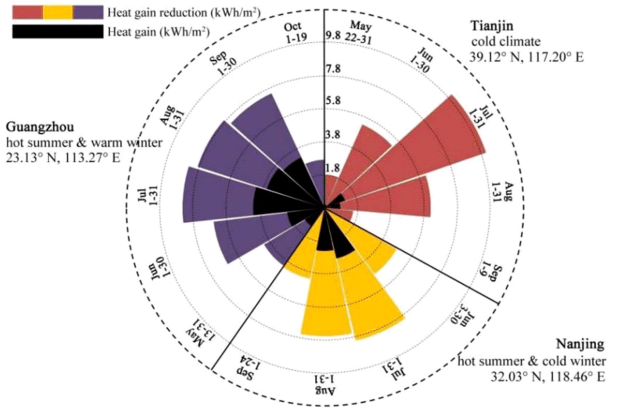

Figure 11. The monthly accumulated heat gain in typical cities.

absorbance. When the pipe-embedded PCM interlayer is added, the influence of solar irradiance is reduced remarkably. And the accumulated heat gain in different orientations is both turned into negative, which means the interior wall surface will take away the heat from the room instead of transferring the environment heat into the room. The simulation results also indicate that due to the differences in primary meteorological conditions in different cities, the cumulative heat gains in the four directions in the same city are slightly different. Obviously, the accumulated heat gain at different orientations in Guangzhou is higher than Tianjin and Nanjing due to a longer cooling season. From the perspective of orientation, because the dark side (i.e., the North) of the building gets less heat and needs less heat reduction to improve indoor thermal comfort, the reduction of cumulative heat gain in the north of the building is relatively less than that of the other three sunny sides, while the south side of the main sunny side gets the most heat, and the reduction effect of cumulative heat gain is very obvious. In a word, it is convincing that PEPCW system is effective in all of the four orientations, especially in the sunny side where the heat gain reduction is greater.

4 Conclusions

The concept of thermo-activated PCM composite wall (PEPCW) is proposed to address the shortcomings existed in traditional energy saving retrofit measures and to solve application challenges of pipe-embedded building envelope facing the vast existing buildings. In this paper, the heat transfer performance of the PEPCW driven by the intermittent high-temperature cold water and its effectiveness in the aspect of energy saving are examined, which is accomplished by using a validated numerical model. Furthermore, the effects of pipe interval, PCM thickness, climate region and the orientation on the thermal behavior and the energy saving and economic potential are also numerically investigated. The main conclusions are as follows: Select three typical cities to study the effects of climate regions and orientations on the thermal behavior and the energy saving and economic potential.

(1) The comparative study between PEPCW and normal wall preliminarily verify the effectiveness of PEPCW in stabilizing the interior surface temperature, offsetting the cold loss through the building envelope and even supplying coldness energy to the indoor space of the existing buildings needed to be retrofitted. With the pipe-embedded PCM system, the temperature and heat flux amplitude of interior surface of PEPCW under Tianjin conditions can be decreased by 1.1 ℃ and 9.9 $W \cdot m^{-2}$, respectively.

(Ⅱ) Results show that the pipe spacing has a more obvious influence than PCM thickness. Considering the cost performance, a thinner PCM layer (e.g., 30 mm) and a larger pipe interval (e.g., 300 mm) is recommended though a closer arrangement of the embedded pipe and a thinner PCM layer shows a smaller accumulated heat gain value.

(Ⅲ) The summer thermal performances of PEPCW

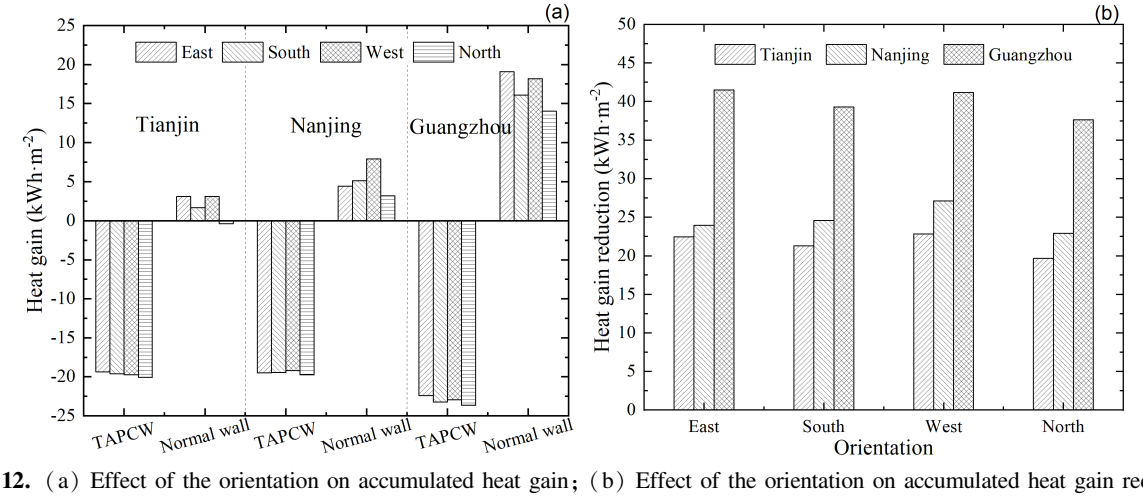

Figure 12. (a) Effect of the orientation on accumulated heat gain; (b) Effect of the orientation on accumulated heat gain reduction.

in retrofitting buildings are proved satisfactory in all the studied three cities. Results show that the maximum heat gain reduction (i. e., 39. 30 kWh · m^{-2}) after applying PEPCW appears in hot summer and warm winter (i. e., Guangzhou).

(Ⅳ) Compared with the static ordinary wall, the influence of solar radiation on the indoor thermal environment could be remarkably reduced. Results show that the PEPCW applied in the three sunny orientations are more effective than the the dark orientation (i. e., north).

The above results and conclusions obtained from numerical research have specific theoretical guiding significance for further research and application of PEPCW. However, there are still several issues that need to be further resolved: (1) Many factors affect the thermal performance of PEPCW, including cold/heat source temperature, installation area, thermal physical parameters of phase change materials, indoor set temperature and existing building enclosure Structural types, etc., need to be further analyzed in conjunction with actual projects; (2) PEPCW systems should be applied to the actual reconstruction of existing buildings In the case, the overall thermal performance of the reconstructed building was experimentally verified and long-term tested, and its application effects were more comprehensively evaluated to give more targeted guidance on the technology.

Acknowledgments

This work is supported by the Youth Fund of Anhui Natural Science Foundation (2108085QE241), National Key Research and Development Program of China (2021YFE0200100), Fundamental Research Funds for the Central Universities (PA2021KCPY0038), Department of Housing and Urban-Rural Development of Anhui Province (2020-YF36) and Anhui Natural Science Research Projects of Universities (KJ2020A0462).

Conflict of interest

The authors declare no conflict of interest.

Author information

CHEN Sarula received her PhD in Architecture from Tianjin University. She is a master supervisor at Anhui Jianzhu University. She is a specialist in building energy-saving and ultra-low energy consumption fields.

YANG Yang (corresponding author) received his PhD in Architecture from Tianjin University. He is a specialist in building energy-saving and ultra-low energy consumption fields.

References

[1] IEA. World Energy Statistics 2020. Paris: International Energy Agency, 2021.

[2] Li N, Liu X, Yu B. The performance analysis on a novel purified PV-Trombe wall for electricity, space heating, formaldehyde degradation and bacteria inactivation. Journal of University of Science and Technology of China, 2021, 51: 308-318.

[3] Ye R, Lin W, Fang X, et al. A numerical study of building integrated with $CaCl_2 \cdot 6H_2O$/ expanded graphite composite phase change material. Applied Thermal Engineering, 2017, 126: 480-488.

[4] MaPugsley A, Zacharopoulos A, Mondol J, et al. Vertical Planar Liquid-Vapour Thermal Diodes (PLVTD) and their application in building facade energy systems. Applied Thermal Engineering, 2020, 179: 115641.

[5] Lodi C, Magli S, Contini F, et al. Improvement of thermal comfort and energy efficiency in historical and monumental buildings by means of localized heating based on non-invasive electric radiant panels. Applied Thermal Engineering, 2017, 126: 276-289.

[6] Ji Y, Fitton R, Swan W, et al. Assessing overheating of the UK existing dwellings-A case study of replica Victorian end terrace house. Building and Environment, 2014, 77: 1-11.

[7] Ye H, Wang Z, Wang L, et al. Effects of PCM on thermal control performance of a thermal control system subjected to periodic ambient conditions. Journal of University of Science and Technology of China, 2016, 46: 845-852.

[8] Yang Z, Zhang Q, Zhang W, et al. Research progress on heat transfer enhancement methods for medium temperature latent heat thermal energy storage systems. Chemical Industry and Engineering Progress, 2019, 38: 4389-4402.

[9] Oliver A. Thermal characterization of gypsum boards with PCM included: Thermal energy storage in buildings through latent heat. Energy and Buildings, 2012, 48: 1-7.

[10] Zhu L, Yang Y, Chen S, et al. Numerical study on the thermal performance of lightweight temporary building integrated with phase change materials. Applied Thermal Engineering, 2018, 138: 35-47.

[11] Vicente R, Silva T. Brick masonry walls with PCM macrocapsules: An experimental approach. Applied Thermal Engineering, 2014, 67: 24-34.

[12] Gholamibozanjani G, Farid M. Application of an active PCM storage system into a building for heating/cooling load reduction. Energy, 2020, 210: 118572.

[13] Rathore P, Shukla S K. An experimental evaluation of thermal behavior of the building envelope using macroencapsulated PCM for energy savings. Renewable Energy, 2020, 149: 1300-1313

[14] Fateh A, Borelli D, Devia F, et al. Summer thermal performances of PCM-integrated insulation layers for light-weight building walls: Effect of orientation and melting point temperature. Thermal Science and Engineering Progress, 2018, 6: 361-369.

[15] Zhu N, Ma Z, Hu P, et al. Energy performance of double shape-stabilized phase change materials wallboards in office building. Applied Thermal Engineering, 2016, 105: 180-188.

[16] Yu N, Chen C, Lin J, et al. Thermal properties of phase change materials used in buildings for solar phase change thermal storage curing of precast concrete components. Chemical Industry and Engineering Progress, 2021, 40: 297-304.

[17] Romani J, Cabeza L, Perez G, et al. Experimental testing of cooling internal loads with a radiant wall. Renewable Energy, 2017, 116: 1-8.
[18] Zhou L, Li C. Study on thermal and energy-saving performances of pipe-embedded wall utilizing low-grade energy. Applied Thermal Engineering, 2020, 176: 115477.
[19] Luo Y, Zhang L, Bozlar M, et al. Active building envelope systems toward renewable and sustainable energy. Renewable and Sustainable Energy Reviews, 2019: 470-491.
[20] Ibrahim M, Wurtz E, Anger J, et al. Experimental and numerical study on a novel low temperature façade solar thermal collector to decrease the heating demands: A south-north pipe-embedded closed-water-loop system. Solar Energy, 2017, 147: 22-36.
[21] Rayegan S, Motaghian S, Heidarinejad G, et al. Dynamic simulation and multi-objective optimization of a solar-assisted desiccant cooling system integrated with ground source renewable energy. Applied Thermal Engineering, 2020, 173: 115210.
[22] Jeong S, Tso C, Zouagui M, et al. A numerical study of daytime passive radiative coolers for space cooling in buildings. Building Simulation, 2018, 11: 1011-1028.
[23] Xie J, Zhu Q, Xu X, et al. An active pipe-embedded building envelope for utilizing low-grade energy sources. Journal of Central South University, 2012, 19: 1663-1667.
[24] Yu Y, Niu F, Guo H, et al. A thermo-activated wall for load reduction and supplementary cooling with free to low-cost thermal water. Energy, 2016, 99: 250-265.
[25] Shen C, Li X, Yan S, et al. Numerical study on energy efficiency and economy of a pipe-embedded glass envelope directly utilizing ground-source water for heating in diverse climates. Energy Conversion and Management, 2017, 150: 878-889.
[26] Jiang S, Li X, Lyu W, et al. Numerical investigation of the energy efficiency of a serial pipe-embedded external wall system considering water temperature changes in the pipeline. Journal of Building Engineering, 2020, 31: 101435.
[27] Prieto A, Knaack U, Auer T, et al. Solar coolfacades: Framework for the integration of solar cooling technologies in the building envelope. Energy, 2017,137: 353-368.
[28] Silvero F, Lops C, Montelpare S, et al. Impact assessment of climate change on buildings in Paraguay—Overheating risk under different future climate scenarios. Building Simulation, 2019, 12: 1-18.
[29] National Development and Reform Commission (NDRC). Opinions on Clean Heating Price Policy in North China. [2021-03-01]. http://www. ndrc. gov. cn/zcfb/zcfbtz/201709/t20170925_861387. html.
[30] Mazo J, Delgado M, Marin J, et al. Modeling a radiant floor system with Phase Change Material (PCM) integrated into a building simulation tool: Analysis of a case study of a floor heating system coupled to a heat pump. Energy and Buildings, 2012, 47: 458-466.
[31] Zhao M, Zhu T, Wang C, et al. Numerical simulation on the thermal performance of hydraulic floor heating system with phase change materials. Applied Thermal Engineering, 2016, 93: 900-907.
[32] B González, Prieto M. Radiant heating floors with PCM bands for thermal energy storage: A numerical analysis. International Journal of Thermal Sciences, 2021, 162: 106803.
[33] Xia Y, Zhang X. Experimental research on a double-layer radiant floor system with phase change material under heating mode. Applied Thermal Engineering, 2016, 96: 600-606.
[34] Fu W, Zou T, Liang X, et al. Thermal properties and thermal conductivity enhancement of composite phase change material using sodium acetate trihydrate-urea/expanded graphite for radiant floor heating system. Applied Thermal Engineering, 2018, 138: 618-626.
[35] Koschenz M, Lehmann B. Development of a thermally activated ceiling panel with PCM for application in lightweight and retrofitted buildings. Energy and Buildings, 2004, 36: 567-578.
[36] Shen C, Li X. Energy saving potential of pipe-embedded building envelope utilizing low-temperature hot water in the heating season. Energy and Building, 2017, 138: 318-31.
[37] Rubitherm. Techdata-RT18HC. [2021-03-01]. https://www. rubitherm. eu/en/.
[38] Ocallaghan P, Probert S. Sol-air temperature. Applied Energy, 1977, 3: 307-311.
[39] Kong X, Lu S, Li Y, et al. Numerical study on the thermal performance of building wall and roof incorporating phase change material panel for passive cooling application. Energy and Buildings, 2014, 81: 404-415.
[40] Nageler P, Schweiger G, Pichler M, et al. Validation of dynamic building energy simulation tools based on a real test-box with thermally activated building systems (TABS). Energy and Buildings, 2018, 168: 42-55.
[41] ANSYS. Ansys Fluent Theory Guide. Canonsburg, PA, 2011.
[42] Faheem A, Ranzi G, Fiorito F, et al. A numerical study on the thermal performance of night ventilated hollow core slabs cast with micro-encapsulated PCM concrete. Energy and Buildings, 2016, 127:892-906.
[43] Du R, Li W, Xiong T, et al. Numerical investigation on the melting of nanoparticle-enhanced PCM in latent heat energy storage unit with spiral coil heat exchanger. Building Simulation, 2019, 12:869-879.
[44] China Academy of Building Research (CABR). Design code for heating ventilation and air conditioning of civil buildings (GB50736-2012). Beijing: China Building Industry Press, 2012.
[45] Blanco J, Arriaga P, Roji E, et al. Investigating the thermal behavior of double-skin perforated sheet façades: Part A: Model characterization and validation procedure. Building and Environment, 2014, 82: 50-62.
[46] China Academy of Building Research (CABR). Code for thermal design of civil buildings (GB50176-2016). Beijing: China Building Industry Press, 2016.
[47] Kharbouch Y, Ouhsaine L, Mimet A, et al. Thermal performance investigation of a PCM-enhanced wall/roof in northern Morocco. Building Simulation, 2018, 11: 1083-1093.
[48] Huo R. Study on thermal storage properties of phase change material wallboard with water-heating system. Beijing: Beijing University of Civil Engineering and Architecture, 2012.

既有建筑嵌管式相变复合墙体夏季热特性研究

陈萨如拉[1,4],常甜馨[1],杨洋[2*],潘超[1],吴运法[1,3,4]

1. 安徽建筑大学建筑与规划学院,安徽合肥 230601
2. 合肥工业大学建筑与艺术学院,安徽合肥 230009
3. 中国科学技术大学火灾科学国家重点实验室,安徽合肥 230027
4. 中国-葡萄牙文化遗产保护科学"一带一路"联合实验室,江苏苏州 215031

* 通讯作者. E-mail:yangyang2017@tju.edu.cn

摘要:管道嵌入式建筑围护结构作为一种重质热激活建筑系统(TABS),由于其管道内嵌于建筑围护结构内部,故目前在既有建筑改造中应用较少.本文提出了管道嵌入式相变复合墙体(PEPCW)的概念,其主要利用基于宏观封装的嵌管式相变板代替传统嵌管夹层,并将嵌管夹层移至承重层外侧,为解决既有建筑改造中应用这一技术提供了创新解决思路.本文利用经实验验证的数学模型评估了PEPCW的夏季热性能和节能潜力,结果表明,复合墙体内表面温度和热流可分别降低1.1℃和9.9 W·m^{-2}.参数化模拟结果表明,管道间距相比相变夹层厚度对复合墙体热性能影响更为明显,所研究条件下的管道间距和相变层厚度建议取值为300/30 mm.通过对三个不同气候分区的典型城市(即天津、南京和广州)开展的应用评估结果还表明,PEPCW在改善室内热舒适度方面可以取得令人满意的效果,尤其是在夏热冬暖地区.此外,应用PEPCW可显著降低太阳辐射吸收率对不同朝向墙体热负荷的影响,三个向阳朝向的指标下降幅度高于北面.综合来看,PEPCW在供冷季节表现出令人满意的热性能,有助于推动嵌管式建筑围护结构在既有建筑中的节能改造应用.

关键词:热性能;TABS;相变材料;数值模型;既有建筑